

Laser-induced fluorescence temperature determination in fuel–air mixtures without additional fluorescence tracers

F. Rotter · J. Scholz · J. Grimsel · H. Wackerbarth ·
V. Beushausen

Received: 25 November 2009 / Revised version: 25 October 2010 / Published online: 25 November 2010
© Springer-Verlag 2010

Abstract A concept for temperature determination of fuel–air mixtures using Laser-Induced Fluorescence (LIF) is presented. For this purpose the fluorescence spectra of gasoline were measured after excitation by frequency quadrupled Nd:YAG laser light at 266 nm in a temperature range between 373 K and 448 K. Experiments were performed with colorless near-standard gasoline conforming to the Euro-super specifications. It is shown that the intensities of two fluorescence bands (290–302 nm and 332–344 nm) can be used to determine the temperature.

1 Introduction

The control of gas mixture formation is essential in many technical applications. For instance, a well defined formation of ignitable hydrocarbon–air mixtures is decisive for an efficient and sustainable energy conversion in combustion engines. The improvement of such combustion processes becomes more and more important due to a rising demand and increasing costs of energy and strengthening of emission constraints. Therefore, many different optical diagno-

tic techniques have been developed during the past decades, aiming to gain an insight into and a better understanding of the processes governing mixture formation [1, 2]. In this context Reboux et al. [3] proposed the measurement of the fuel–air ratio by so called Fuel-Air-Ratio Laser-Induced Fluorescence (FARLIF) as a promising approach more than 10 years ago. They used toluene as a fluorescence tracer in the model fuel iso-octane and an excitation wavelength of 248 nm. It was shown that the fluorescence intensity grows linearly with the fuel–air ratio at ambient temperature.

In the following years, this technique was used by many research groups even at elevated temperatures without being tested for applicability. However, Schulz and Sick concluded from their investigations that the applicability of the FARLIF concept is questionable at high temperatures and an excitation wavelength of 248 nm [4]. Koban et al. presented results indicating an applicability of the FARLIF concept at longer excitation wavelengths (e.g. 266 nm) and temperatures up to 500 K [5, 6], but their experiments were limited to a total pressure of 0.1 MPa. Scholz et al. systematically examined the FARLIF concept for elevated temperatures and pressures and, therefore, a parameter regime, which is more relevant to combustion analysis [7–9]. They were able to validate it for toluene as a fluorescence tracer in iso-octane [7], a commonly used model fuel, and for auto-fluorescing near-standard gasoline without any additional tracer for temperatures up to 548 K [7–9]. However, they found a temperature dependence of the proportionality factor of the FARLIF intensity [8]. Therefore, quantitative measurements of the fuel–air ratio demand exact knowledge of the temperature of the gas mixture inside the detection volume. Quantitative measurements under conditions with inhomogeneous unknown temperature distributions are impossible. To enable temperature correction of FARLIF data this paper introduces a temperature measurement strategy

F. Rotter (✉) · J. Scholz · J. Grimsel · H. Wackerbarth ·
V. Beushausen
Laser Laboratorium e.V., Hans-Adolf-Krebs-Weg 1,
37077 Göttingen, Germany
e-mail: frank.rotter@llg-ev.de

J. Scholz
Currently with the Sartorius AG, R&D Lab Instruments
Analytics, Weender Landstraße 94–108, 37075 Göttingen,
Germany

J. Grimsel
Currently with the Musterschule Frankfurt am Main, Oberweg
5–9, 60318 Frankfurt am Main, Germany

utilizing two temperature sensitive fluorescence bands of aromatic hydrocarbons, which are inherently present in standard gasoline.

2 The FARLIF concept

The FARLIF concept is feasible in the case of linear LIF (weak excitation). In this case the fluorescence intensity I_f is proportional to the number density of the fluorophore n_f and the fluorescence quantum yield q_f . In the case of collisional quenching by oxygen as the dominant fluorescence deactivation process, I_f can be described by

$$I_f \propto q_f n_f = \frac{k_{\text{rad}}}{k_f + k_{qO_2} n_{O_2}} n_f. \quad (1)$$

I_f depends on the coefficient for spontaneous emission k_{rad} , the assembled coefficient for intra-molecular deactivation processes k_f , the oxygen quenching coefficient k_{qO_2} and the number density of oxygen n_{O_2} . If the oxygen quenching dominates the intra-molecular deactivation processes, i.e. if $k_f \ll k_{qO_2} n_{O_2}$, k_f can be neglected and the fluorescence intensity becomes proportional to the ratio of fluorophore and oxygen:

$$I_f \propto \frac{k_{\text{rad}}}{k_{qO_2}} \frac{n_f}{n_{O_2}}. \quad (2)$$

This means that with rising pressure the FARLIF signal becomes pressure independent and proportional to the mixture ratio n_f/n_{O_2} which is again proportional to the equivalence ratio $\phi = 1/\lambda$, where the λ -value denotes the stoichiometric air-fuel ratio (for stoichiometric mixtures $\lambda = 1$, ignitable mixtures have $0.5 < \lambda < 1.3$).

3 Experimental part

With the aim to find a strategy for temperature determination and correction in the context of FARLIF measurements, spectral information of the fluorescence was evaluated. For this purpose, fluorescence spectra of gaseous fuel-air mixtures were recorded at different gas temperatures inside a heatable pressure chamber. Quartz glass windows enabled light transmission through the chamber. A frequency quadrupled Nd:YAG laser emitting light pulses at 266 nm was used for excitation. The excitation light was formed to a light sheet of 1 mm by 25 mm by means of cylinder lenses. The fluorescence light was focused to the slit of an in-house built grating spectrometer, which was equipped with a 1200 lines/mm grating and an intensified CCD camera as detector. Figure 1 shows the measurement setup.

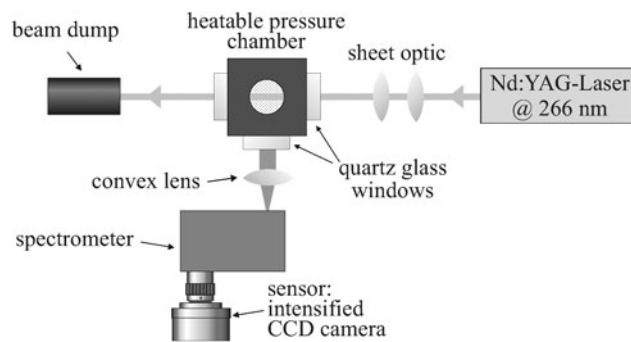


Fig. 1 Scheme of the fluorescence measurement setup

Table 1 Fuel partial-pressure corresponding to the fuel density of 9.1×10^{18} molecules m $^{-3}$ at different temperatures

| Temperature (K) | 373 | 398 | 423 | 448 |
|------------------------|-----|-----|-----|-----|
| Partial pressure (kPa) | 4.7 | 5.0 | 5.3 | 5.6 |

Experiments were conducted with “Shell colorless gasoline” (PR 1632), which is a special multi-component fuel, conforming to the Euro-super specifications. But, in contrast to standard filling station blends, it does not include the yellow-brownish bitumen components in order to prevent window fouling. In contrast to model fuels, the usage of this near-standard gasoline enables more realistic engine experiments. In addition, “Shell colorless gasoline” contains aromatic compounds and, therefore, is auto-fluorescing, whereby it allows experiments without additional tracers.

Fuel-air mixtures were prepared in a heated 500 ml reservoir. After injecting the fuel, the reservoir was filled up with synthetic air, consisting of 20 percent oxygen and 80 percent nitrogen to get the required mole fraction. To obtain a homogeneous mixture by diffusion, the gas was left in the reservoir for 20 minutes. A heated pipe system with bellow-sealed valves allowed the charging of the pressure chamber with the prepared mixture.

In all experiments measurements were conducted using a fuel density of 9.1×10^{18} molecules m $^{-3}$. Pressure gauges enabled control of the fuel and air partial pressure and, thereby, of the density. Table 1 shows the pressure values used as calculated with the ideal gas law. Fuel-air mixtures of the gasoline used are stoichiometric at a 1:50 ratio. This means that a $\lambda = 1$ mixture under the experimental conditions used has an air partial pressure of about 0.25 MPa. Scholz et al. infer from their studies that the FARLIF concept is applicable within a 5% error limit at pressures above 0.25 MPa, with sufficient air fraction ($\lambda \geq 0.4$) and temperatures up to 548 K. At lower temperatures both the pressure and the air fraction may be reduced for FARLIF applications [8]. Thus, the experiments were mainly conducted under conditions where FARLIF becomes valid.

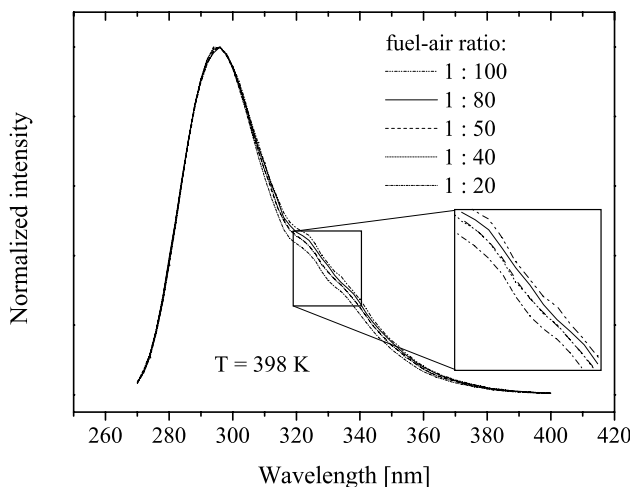


Fig. 2 Fluorescence spectra of different mixtures of “Shell colorless gasoline” and synthetic air. The spectra are normalized to their maximum

4 Results and discussion

Figure 2 shows fluorescence spectra of different mixtures of “Shell colorless gasoline” with synthetic air at 398 K. Each spectrum shows a fluorescence intensity peak at a wavelength of approximately 295 nm. The spectra are normalized to this peak. Furthermore, the spectra show a second fluorescence band at a wavelength of approximately 330 nm overlapping the 295 nm band. The intensity of the long-wavelength band grows with rising air fraction relative to the short-wavelength band.

The integrated intensities of the spectra in Fig. 2 and additional spectra recorded at two different temperatures (425 K and 448 K) in dependence on the equivalence ratio are depicted in Fig. 3. A linear growth can be observed. At a given temperature the slope of the line indicates the calibration for equivalence–ratio measurements. It is obvious that the calibration depends on temperature. The slope grows with rising temperature. Therefore, a measurement strategy for temperature is required. It stands out that the intensity at the equivalence ratio of 2.5 is lower than expected from a linear equivalence–ratio dependence. This is the mixture with a fuel–air ratio of 1:20. Due to the fuel partial pressure of 5.0 kPa the total pressure is about 0.1 MPa and, therefore, below the regime where FARLIF is valid [8].

To gain information about the temperature dependence of the fluorescence, the fluorescence spectra at different temperatures were analyzed in detail. Figure 4 shows the spectra for a nearly stoichiometric mixture at different temperatures. The spectra are normalized to their intensity maximum. It can be observed that the intensity of the second fluorescence band at approximately 330 nm increases with rising temperature, relative to the intensity of the fluorescence maximum at 295 nm. These two fluorescence features

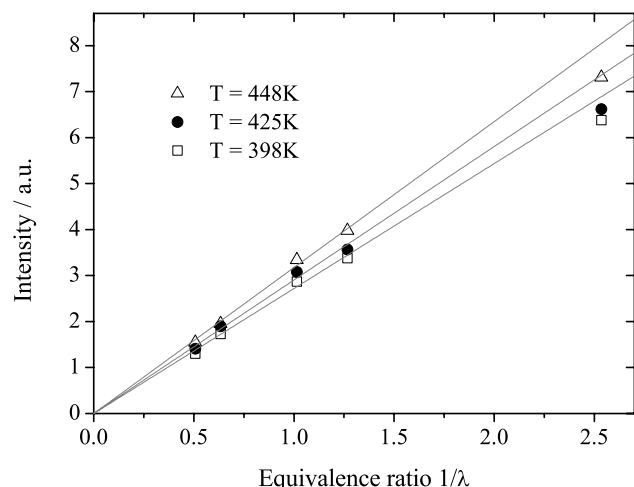


Fig. 3 Fuel–air ratio calibration lines of fluorescence intensity at different temperatures

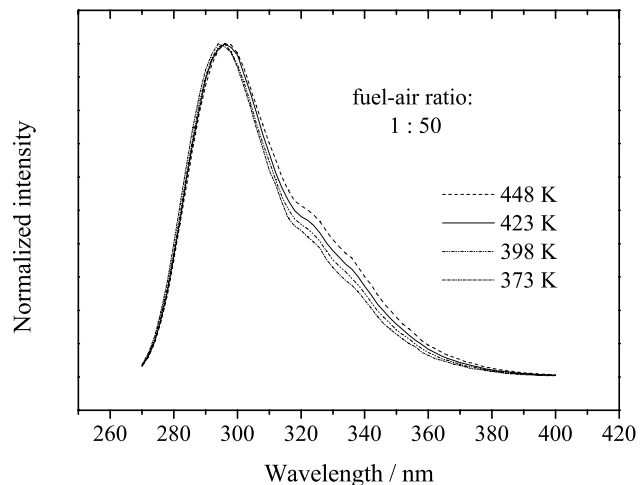


Fig. 4 Temperature dependence of fluorescence spectra of “Shell colorless gasoline”. The spectra are normalized to their maximum

probably originate from two different groups of fluorescing components of the fuel: monoaromatic hydrocarbons, which have a short-wavelength fluorescence band (approx. 270–320 nm), and di aromatics and tri aromatics (in the following referred to as poly aromatics), which have a long-wavelength fluorescence band (approx. 310–380 nm). The fluorescence of the mono aromatics and poly aromatics has a different temperature dependence. This observation is in accordance with analogous data on kerosene fluorescence [10, 11]. But compared with the results of these publications, in the case of “Shell colorless gasoline” the poly aromatics fluorescence is much weaker than the mono aromatics fluorescence. The reason for this can be found in the poly aromatics mole fraction, which, in contrast to kerosene, is very small in gasoline.

To support the thesis that the different fluorescence bands originate from different aromatic hydrocarbon components

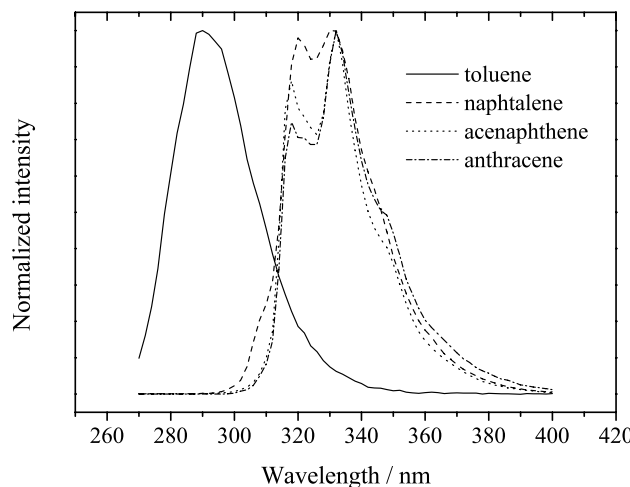


Fig. 5 Normalized spectra of different aromatic hydrocarbons

of the fuel, spectra of pure aromatic hydrocarbons, solved in non-fluorescent isoctane and evaporated at a pressure of 5.0 kPa and a temperature of 398 K, were recorded on the basis of the work described in [10, 11]. The spectra of toluene as monoaromatic hydrocarbon, naphthalene, acenaphthene and anthracene as polyaromatic hydrocarbons are plotted in Fig. 5. Toluene shows a fluorescence peak at 290 nm, while the other hydrocarbons exhibit very distinct fluorescence around 330 nm. This coincides with the features observed in the gasoline spectra, which is in accordance with the assumption that the structure of the gasoline fluorescence spectra results from such components.

Based on the different temperature behaviors of the monoaromatics and polyaromatics a temperature measurement strategy can be developed that makes use of the intensity ratio of both fluorescence bands. In order to test if this strategy is applicable for FARLIF measurements, two wavelength ranges in the spectra were defined: 290–302 nm and 332–344 nm. The fluorescence intensity (S_1 and S_2 , respectively) was integrated for each spectral range and the temperature dependence of the intensity ratio S_1/S_2 was analyzed. In Fig. 6 the intensity ratio S_1/S_2 of “Shell colorless gasoline” is plotted against the temperature for different fuel-air mixtures with ratios between 1:20 and 1:100 in the temperature range from 373 K to 448 K. For each mixture, the intensity ratio shows an almost linear temperature dependence. Therefore, the broadband detection of the two fluorescence bands can be used for temperature measurement in gaseous fuel-air mixtures.

The intensity ratio of two wavelength bands was used by other groups to gain temperature information from the fluorescence of a single aromatic hydrocarbon as tracer, e.g. Kaiser et al. used naphthalenes [12], Orain et al. used 1,2,4-trimethylbenzene [13] and Luong et al. used toluene [14]. These groups observed a slight red shift of the fluorescence

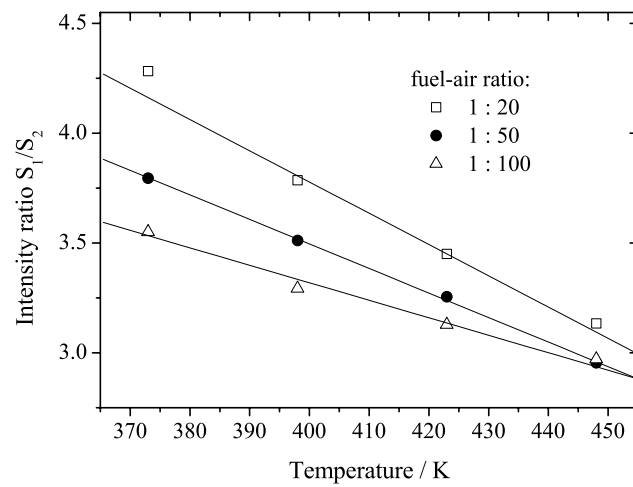


Fig. 6 Temperature dependence of the intensity ratio S_1/S_2 of the monoaromatics and diaromatics in “Shell colorless gasoline”

spectra with rising temperature, while other parameters like pressure and oxygen concentration have no or little influence on the shape of the spectra. Though, the authors also report a strong dependence of the fluorescence intensity on the temperature and on the oxygen concentration, due to quenching. This intensity variation cancels by using the intensity ratio of two wavelength bands. This ratio then gives a measure for the red shift and this, in turn, gives the temperature.

In the present work the used spectral bands were chosen around the maximum fluorescence intensity of monoaromatics and polyaromatics, respectively. The different temperature dependences of the present species’ fluorescence result in a temperature dependent intensity ratio, which is used for temperature measurement. Since the fluorescence spectra of these two tracer groups overlap slightly, the intensity ratio is also influenced by the temperature dependent red shift of the single spectra. However, this influence amplifies the sensitivity of the method, because both, the red shift and the relative growth of the polyaromatics fluorescence intensity with rising temperature, results in an increase of the long-wavelength band.

In contrast to the single-tracer temperature determination which benefits from the oxygen invariance of the fluorescence spectra, the temperature measurement with “Shell colorless gasoline” unfortunately is influenced by oxygen. This means the temperature calibration of the S_1/S_2 ratio varies with the fuel-air ratio, as can be seen in Fig. 6. The reason for this is the different quenching behavior of the two tracer groups, monoaromatics and polyaromatics, which causes a dependence of the shape of the fluorescence spectrum of the gasoline on the oxygen concentration. The different quenching behavior of monoaromatics and diaromatics can be observed in Fig. 7. There, Baranger et al. [10] plotted I_0/I of kerosene over the molar oxygen fraction X_{O_2} . I is the oxygen dependent fluorescence intensity and I_0 is the fluores-

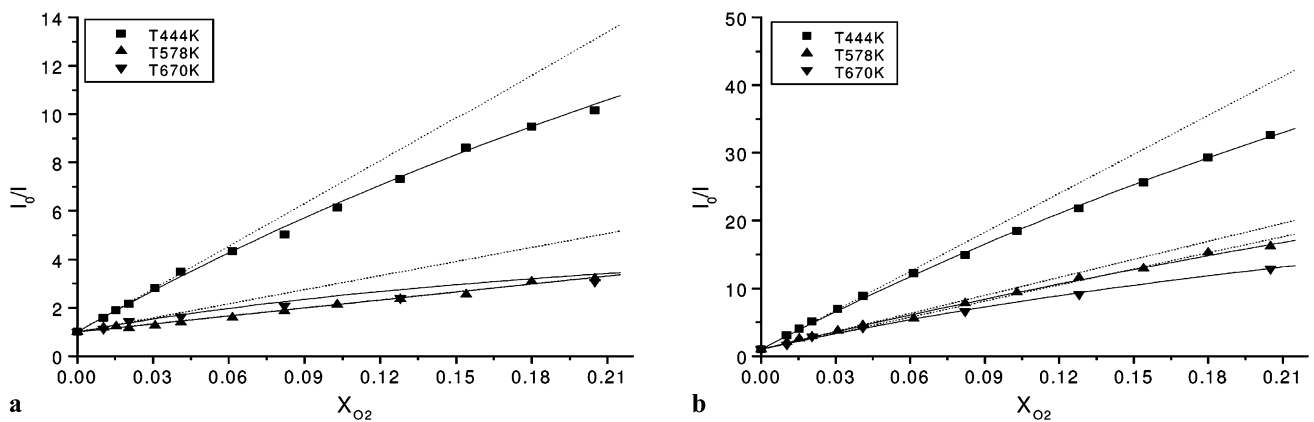


Fig. 7 Kerosene fluorescence as a function of molar fraction of oxygen at 0.1 MPa for various temperatures: (a) fluorescence of the 270–310 nm band, (b) fluorescence of the 310–420 nm band. Reprinted from [10] with permission of the American Institute of Aeronautics and Astronautics

cence intensity without oxygen presence. Part (a) shows the fluorescence of the 270–310 nm band, which is associated to monoaromatics, while part (b) shows the fluorescence of the 310–420 nm band, which originates mainly from diaromatics. It is obvious that the I_0/I variation of the diaromatics is much higher than the I_0/I variation of the monoaromatics.

This means the proposed technique can be used directly for temperature determination at a constant fuel-air ratio. In mixtures, where the fuel-air ratio as well as temperature are unknown or inhomogeneous, both parameters can be extracted from the fluorescence.

However, in contrast to the single-tracer temperature determination “Shell colorless gasoline” has the advantage to be more realistic in mixing and combustion behavior and, therefore, allows observations with more relevance for standard gasoline combustion than model fuels.

5 Conclusion

The fluorescence spectra of gaseous fuel with admixtures of synthetic air in the range from 1:20 to 1:100 and at temperatures between 373 K and 448 K were acquired. It was shown that the fluorescence intensity gives information about the fuel-air ratio and the intensity fraction of two different wavelength bands can be used to gain temperature information. Here, a cross sensitivity of the calibration of fuel-air ratio measurement and temperature determination arose. Thus, for measurements under conditions where both fuel-air ratio and temperature are inhomogeneous or unknown, these target values can be calculated using an iterative algorithm or a look-up table, for example. Further investigations concerning this point are in progress to develop an integrated fuel-air ratio and temperature measurement

concept. However, utilizing this new measurement principle, even planar gas-temperature measurements are possible by the use of two CCD cameras, each camera equipped with an appropriate spectral filter for the spectral range S1 and S2, respectively, which record the same detection volume.

Acknowledgements The authors gratefully acknowledge the financial support of the “Deutsche Forschungsgemeinschaft DFG” in the framework of the priority program SPP 1147.

References

1. M.C. Drake, D.C. Haworth, Proc. Combust. Inst. **31**, 99 (2007)
2. A. Grosch, V. Beushausen, H. Wackerbarth, O. Thiele, T. Berg, Appl. Opt. **49**, 196 (2010)
3. J. Reboux, D. Puechberty, F. Dionnet, S.A.E. Tech. Paper Ser., No. 941988 (1994)
4. C. Schulz, V. Sick, Prog. Energy Combust. Sci. **31**, 75 (2005)
5. W. Koban, J. Koch, R. Hanson, C. Schulz, Appl. Phys. B **80**, 777 (2005)
6. W. Koban, J. Koch, R. Hanson, C. Schulz, Appl. Phys. B **80**, 147 (2005)
7. J. Scholz, M. Röhl, T. Wiersbinski, V. Beushausen, In: 13th International Symposium on Applications of Laser Techniques to Fluid Mechanics, Lisbon (2006)
8. J. Scholz, T. Wiersbinski, V. Beushausen, S.A.E. Paper, 2007-01-0645 (2007)
9. J. Scholz, T. Wiersbinski, P. Ruhnau, D. Kondermann, C. Garbe, R. Hain, V. Beushausen, Exp. Fluids **45**, 583 (2008)
10. P. Baranger, M. Orain, F. Grisch, In: 43rd AAIA Aerospace Sciences Meeting and Exhibit, Reno, Nevada, Paper No. 2005-828 (2005)
11. B. Rossow, M. Orain, F. Grisch, In: *12th International Symposium on Flow Visualisation*, Göttingen (2006)
12. S.A. Kaiser, M.B. Long, Proc. Combust. Inst. **30**, 1555 (2005)
13. M. Orain, P. Baranger, B. Rossow, F. Grisch, Appl. Phys. B **100**, 945 (2010)
14. M. Luong, R. Zhang, C. Schulz, V. Sick, Appl. Phys. B **91**, 669 (2008)